ACS OMEGA

Article

Cite This: ACS Omega 2019, 4, 8299−8304

http://pubs.acs.org/journal/acsodf

Water−Organic Cosolvent Effect on Nucleation of Solution-Synthesized ZnO Nanowires

Yuya Akihiro,[†] Kazuki Nagashima,*[,†] Takuro Hosomi,[†] Masaki Kanai,[†] Hiroshi Anzai,[†] Tsunaki Takahashi,[†] Guozhu Zhang,[†] Takao Yasui,[‡] Yoshinobu Baba,[‡] and Takeshi Yanagida*[,†]

[†]Institute for Materials Chemistry and Engineering, Kyushu University, 6-1 Kasuga-Koen, Kasuga, Fukuoka 816-8580, Japan

[‡]Department of Biomolecular Engineering, Graduate School of Engineering, Nagoya University, Furo-cho, Chikusa-ku, Nagoya 464-8603, Japan

ABSTRACT: Here, we show the effect of water−organic (acetone, *tert*-butyl alcohol, and isopropanol) cosolvents on nucleation and anisotropic crystal growth of solution-synthesized ZnO nanowires. The addition of organic solution does not alter the face-selective crystal growth nature but significantly promotes the crystal growth of both length and diameter of the nanowires. Systematic investigations reveal that a variation of the relative dielectric constant in the cosolvent can rigorously explain the observed effect of the water−organic cosolvent on the ZnO nanowire growth via the degree of supersaturation for the nucleation. The difference between acetone, *tert*-butyl alcohol, and isopropanol on the cosolvent effect can be interpreted in terms of a local solvent-sorting effect.

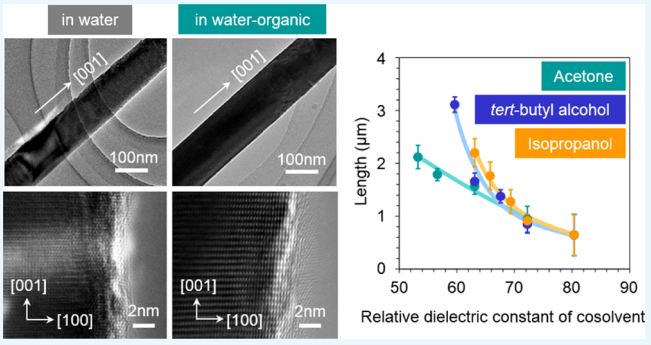

INTRODUCTION

Single crystalline metal oxide nanowires (e.g., ZnO, TiO_2, and WO_3) grown by a low-temperature solution synthesis have been spotlighted in both fundamental science and device applications[1−7] due to the attractive features of metal oxides such as thermal/chemical stabilities in air/water[8] and various functionalities (e.g., wide bandgap, piezoelectricity, photocatalytic effect, and electrochromism).[9−12] The most remarkable feature of the solution synthesis is that the fabrication process can be operated at temperatures less than 100 °C,[13] which is hardly attainable for a high-temperature vapor-phase nanowire synthesis.[14,15] To date, the solution-based nanowire growths have been intensively investigated and various strategies using the counter ions,[16] the ligand-exchange effect,[17] and the surfactant-induced surface capping[18−20] have been successfully demonstrated to tailor the nanowire growth together with an in-depth understanding of the crystal growth mechanism. These solution-based nanowire syntheses normally employ water-soluble chemicals.[1−12,16−20] The use of a water−organic cosolvent (e.g., acetone and alcohol) is one promising way to expand the range of available chemical reagents by increasing the solubility of water-insoluble chemicals.[21,22] This would open up a new strategy to design the nanowire growth with the functional properties of organic chemical reagents. There are many reports as for the synthesis of metal oxide nanostructures in organic solvents and water−organic and organic−organic cosolvents, and the significant changes in their morphologies were demonstrated by using different solvents.[23−26] However, the nanowire growth in a water−organic cosolvent is poorly understood because of the inherent difficulties in understanding the role of the organic solvent by eliminating the concomitant pressure variation and in evaluating the complex chemical interactions between the solutes and solvents. For example, the pressure inside the autoclave system is varied when using different organic solvents and mixing ratios in the conventional hydrothermal and solvothermal growths. Furthermore, the growth parameters such as pH values and concentrations of the ionic species, which give important information to understand the crystal growth mechanism in the water system, are ambiguous in the water−organic cosolvent system. These issues should be overcome to explore the growth mechanism of metal oxide nanowires in the water−organic cosolvent. In our previous study, we investigated the solution growth of zinc oxide (ZnO) nanowires on a viewpoint of nucleation phenomena and successfully explained their anisotropic crystal growth mechanism via a competition of nucleation events on the (0001) plane and (10$\bar{1}$0) plane.[27] These findings clearly show that an analytical approach based on the nucleation theory gives us lots of important information for understanding the solution-based nanowire growths, as primarily demonstrated in the vapor-phase nanowire synthesis.[14,15,28,29] Because this approach is independent from the properties of employed chemical

Received: April 3, 2019
Accepted: April 30, 2019
Published: May 8, 2019

DOI: 10.1021/acsomega.9b00945
ACS Omega 2019, 4, 8299−8304

reagents, it considerably helps to understand the nanowire growth in the water−organic cosolvent.

Here, we investigate the solution based synthesis of ZnO nanowires in various water−organic cosolvents (e.g., acetone, *tert*-butyl alcohol, and isopropanol) by systematically varying their mixing ratio. In order to eliminate the pressure change in different water−organic cosolvent systems, we employed the open growth system in this study, which is different from a conventional closed system like autoclave.[23−26] On the basis of the nucleation theory, we discuss the effects of an organic solvent in terms of the critical nucleation concentration, the temperature change, the liquid−solid interfacial energy, and the solubility related supersaturation.

RESULTS AND DISCUSSION

Figure 1a shows the field emission scanning electron microscopy (FESEM) images of ZnO nanowires grown in the water−acetone cosolvent when varying the mixing ratio. The Zn concentration of 25 mM was first prepared in 100 mL water prior to the acetone addition, and therefore the concentration of the Zn precursor in the solution was diluted by the addition of acetone. We found that both the length and the diameter of ZnO nanowires tended to increase when increasing the amount of acetone addition. These trends can be more clearly seen in Figure 1b, statistically analyzed length and diameter data of ZnO nanowires as a function of the amount of acetone addition. The acetone addition promotes the crystal growths on both (0001) and (10$\bar{1}$0) planes. Note that the increase of Zn concentration via evaporation of the water−organic cosolvent can be neglected because the remaining solvent volume was not less than that of used water after the growth. Figure 2a shows the transmission electron microscopy (TEM) images of ZnO nanowires grown in the water (acetone 0 mL) or water−acetone (acetone 50 mL) cosolvent. There is no significant difference between the two in the surface structure, the single crystallinity, and the growth orientation along [0001]. The preserved growth orientation along [0001] was also confirmed by the X-ray diffraction (XRD) data shown in Figure 2b. Figure 2c shows the room temperature photoluminescence (PL) data of the ZnO nanowires grown in both water-based and water−acetone mixed solvents. Only a slight change in the intensity of the defect-related peak was observed around 610 nm by the acetone addition, and any other variation of optical properties was not seen as the wavelengths of both the near-band-edge (NBE) emission peak and the defect-related peak were maintained. Thus, the acetone addition does not significantly modify the properties of ZnO nanowires within the range of current experiments.

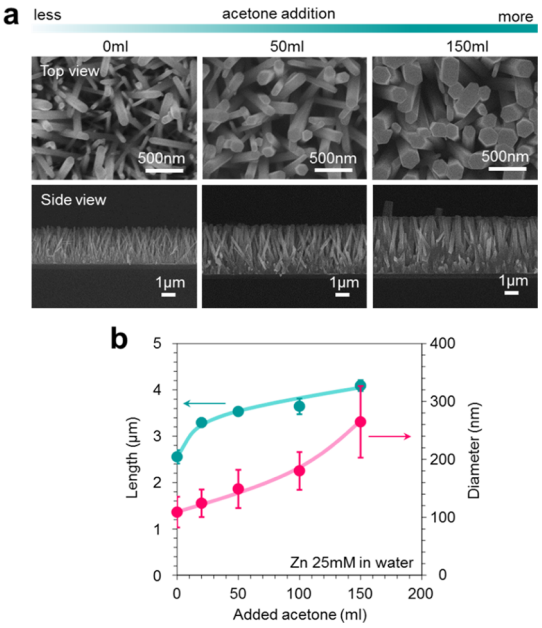

Figure 1. (a) Top view and side view FESEM images of ZnO nanowires grown in the water−acetone mixed solvent with varying the amount of acetone addition (0, 50 and 150 mL). (b) Statistically analyzed data of length and diameter of ZnO nanowires with varying the amount of acetone addition. The Zn concentration was controlled to be 25 mM in water prior to the acetone addition.

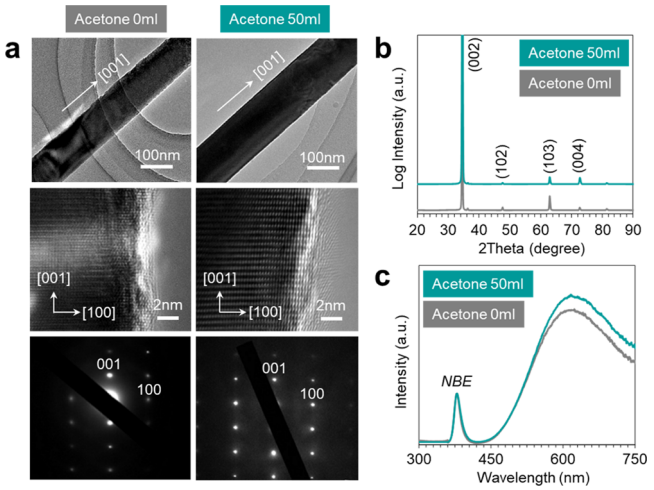

Figure 2. (a) Low magnification TEM images (upper), high magnification TEM images (middle), and SAED patterns (lower) of ZnO nanowires grown in water-based (acetone 0 mL: left) and water−acetone mixed (acetone 50 mL: right) solvents. (b) XRD patterns and (c) room temperature PL of ZnO nanowires grown in water-based (acetone 0 mL: grey) and water−acetone mixed (acetone 50 mL: green) solvents. NBE denotes near band edge emission. The Zn concentrations of all samples were controlled to be 25 mM in water prior to the acetone addition.

Next, we focus on a nucleation phenomenon to examine the effect of acetone addition on the ZnO nanowire growths by varying the Zn concentration. Previously our study revealed that there are two different critical concentrations of the Zn precursor for initiating a nucleation on both (0001) and (10$\bar{1}$0) planes of ZnO nanowires.[27] The critical concentration for the (0001) plane is always lower than that of the (10$\bar{1}$0) plane, which is an essential requirement for an anisotropic nanowire growth. Measuring the two critical concentrations enables to evaluate the contribution of acetone addition on the initial nucleation on each plane. Figure 3 shows (a) the representative FESEM images, statistically analyzed (b) length, and (c) diameter data of ZnO nanowires grown in the water (acetone 0 mL) or water−acetone (acetone 50 mL) cosolvent by varying the Zn concentration. As can be seen, the acetone addition similarly lowers the critical concentrations of both (0001) and (10$\bar{1}$0) planes, which are marked as triangle symbols in the figures. Thus, the observed acetone addition effect on the nucleation event is not a face-selective event.

DOI: 10.1021/acsomega.9b00945
ACS Omega 2019, 4, 8299−8304

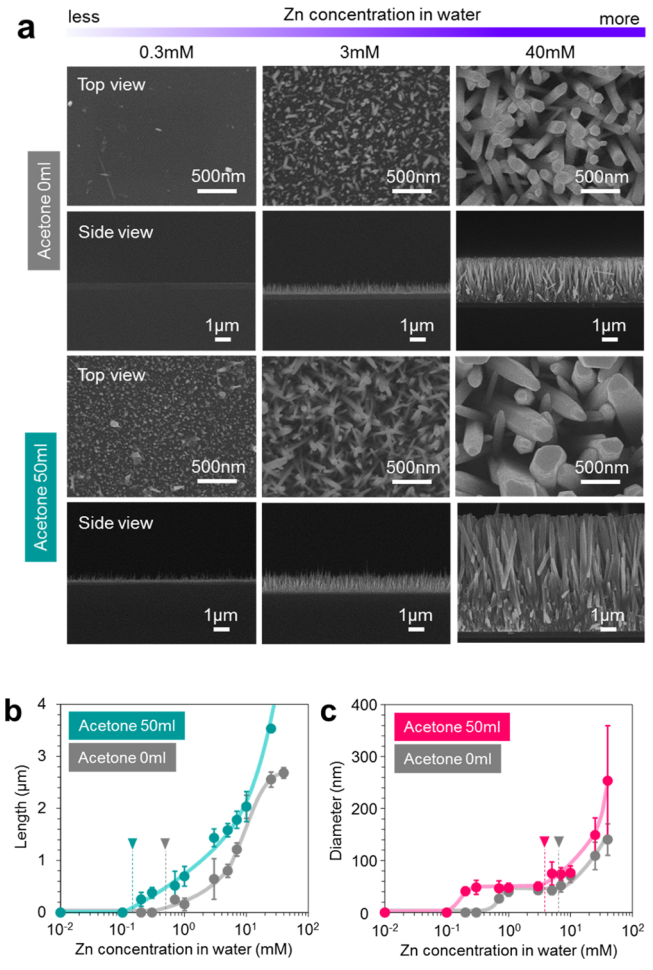

Figure 3. (a) Top view and side view FESEM images of ZnO nanowires grown in water-based (acetone 0 mL: upper) and water–acetone mixed (acetone 50 mL: lower) solvents with varying Zn concentrations (Zn 0.3, 3, and 40 mM). (b,c) Statistically analyzed data of (b) length and (c) diameter of ZnO nanowires grown in water-based (acetone 0 mL: grey) and water–acetone mixed (acetone 50 mL: green & pink) solvents with varying Zn concentrations. The Zn concentration conditions marked with triangle symbols indicate the critical concentrations for nucleation. The Zn concentrations of all samples were calculated prior to the acetone addition.

On the basis of the two dimensional nucleation theory, the rate of crystal growth J can be described as the following equation: $J \propto \exp\left(-\frac{\gamma^2}{4\Delta\mu T}\right)$, where γ is the interfacial energy at the liquid–solid interface, $\Delta\mu$ is the degree of supersaturation and T is the temperature, respectively.[29] According to this, we consider the following three factors including (i) a growth temperature, (ii) an interfacial energy, and (iii) a supersaturation. First, we consider the temperature variation of the growth solution by acetone addition. Figure 4a shows the monitored temperatures of growth solutions during the nanowire growth process. The maximum temperature of 50 mL acetone mixed solvent was 10 °C higher than that of the water solvent. However, this effect was found to be negligible as confirmed by the experiments when increasing the growth temperature in (Figure 4b). Next, we consider the change of interfacial energy at the solvent/ZnO interface by acetone addition because the crystal growth must be promoted with decreasing the interfacial energy γ. To examine the acetone-induced variation of interfacial energy at the solvent/ZnO interface, we measured the contact angle (CA) of the water–acetone cosolvent on the ZnO surface with varying the amount of acetone addition, as shown in Figure 5a (a snapshot of the

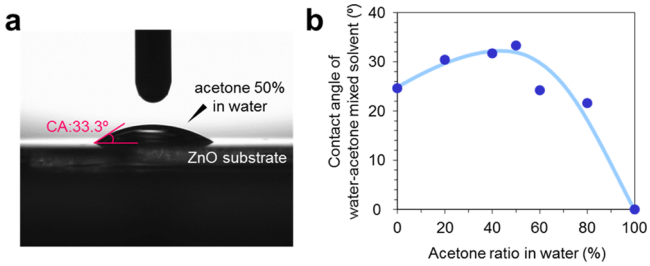

Figure 5. (a) Typical snapshot and (b) static CAs of water–organic mixed solvent dropped onto single crystalline ZnO substrates with varying the mixing ratio of water/acetone. The CA was measured at 10 s after depositing the droplet.

solvent (water/acetone = 50:50%)/ZnO interface and (b) variation of CA with varying the acetone ratio). We found that the CA of the water–acetone cosolvent increased from 24.6° to 33.3° when we varied the acetone ratio in the water–acetone cosolvent from 0 to 50%, and further increase of the acetone ratio resulted in the decrease of the CA. Typically, the

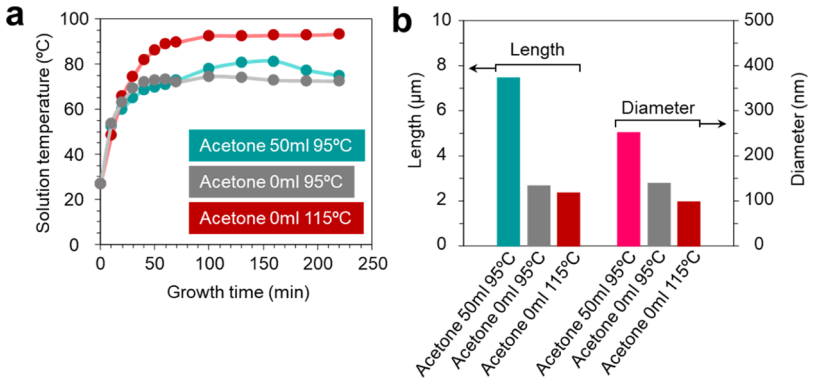

Figure 4. (a) Time dependent temperature variation of growth solution when changing the amount of acetone addition and the programmed temperature of the oven. (b) Comparison of statistically analyzed length and diameter of ZnO nanowires grown by different acetone addition conditions and growth temperatures.

DOI: 10.1021/acsomega.9b00945
ACS Omega 2019, 4, 8299–8304

CA θ is expressed by the following equation: $\cos\theta = (\gamma_{SV} - \gamma_{LS})/\gamma_{VL}$, where γ_{SV}, γ_{LS}, and γ_{VL} are interfacial free energies at solid−vapor, liquid−solid, and vapor−solid interfaces, respectively.[27] Because γ_{VL} should monotonically decrease with increasing acetone ratio due to the lower surface energy of acetone than water, the observed trend of CA at low acetone mixing ratios must be caused by the increase of solvent/ZnO interfacial energy γ_{LS}. This should lead to the suppression of crystal growth. Therefore, the observed acetone addition effect in Figures 1 and 3 cannot be explained in terms of the change of interfacial energy. Finally, we discuss the remaining possible factor for enhancing the crystal growth that is the supersaturation. Because the solubility of ionic substances is strongly dependent on an electrostatic interaction with the solvent,[32] a decrease of the relative dielectric constant in a growth solution may increase the degree of supersaturation of the ionic precursor. Especially in the case of the water−acetone cosolvent, the relative dielectric constant of the growth solution should decrease by increasing the acetone ratio due to the smaller relative dielectric constant of acetone than that of water (acetone: 20.7, water: 78.3 at 25 °C). This might decrease the solubility of Zn-related ionic species, which increases the degree of supersaturation. Figure 6 shows (a) the representative FESEM images, statistically analyzed (b) length, and (c) diameter data of ZnO nanowires grown in water−acetone cosolvents, displayed as a function of the relative dielectric constant of the solvent. As a comparison, the results of water−*tert*-butyl alcohol and water−isopropanol cosolvents are also shown. In these experiments, the Zn concentration of 3 mM was employed to clearly observe the effects of organic addition. In Figure 6, the clear relative dielectric constant dependences on ZnO nanowire growth were commonly observed in both length and diameter data for all cosolvent systems. These results are consistent with the prediction based on the solubility-induced change in the degree of supersaturation and therefore indicate the validity of the model. It is worth noting that the observed trends were contradictory to the previous study conducted using an autoclave by Wen et al. of which the ZnO crystal growth on the (0001) plane was suppressed with increasing the water ratio in the water−ethanol cosolvent,[23] implying that our results were obtained as a consequence of eliminating the pressure change.

Furthermore, we found that the relative dielectric constant dependence becomes stronger in the following order: *tert*-butyl alcohol ≈ isopropanol > acetone. The weaker relative dielectric constant dependence in the water−acetone cosolvent is plausibly because of the formation of the local high relative dielectric constant field around the metal ions by the so-called as "solvent sorting effect".[33,34] Water molecules preferentially interact with metal ions rather than interact with organic solvent molecules the local concentration of water molecules around the metal ions and increase if the hydration energy of the organic solvent molecule is sufficiently low. The increased water concentration increases the solubility of the ionic substance, leading to the decrease of the degree of supersaturation. Considering the lower hydration energy of acetone (45.6 kJ/mol) than *tert*-butyl alcohol (60.4 kJ/mol), and isopropanol (56.3 kJ/mol),[35] the larger solvent sorting effect would be expected in the water−acetone cosolvent. In fact, a smaller solvent sorting effect in the water−alcohol cosolvent than in the water−acetone cosolvent was reported.[33] Thus, these results consistently highlight the crucial importance of the relative dielectric constant of the solvent for the nucleation event on ZnO nanowire growths in water−organic cosolvents.

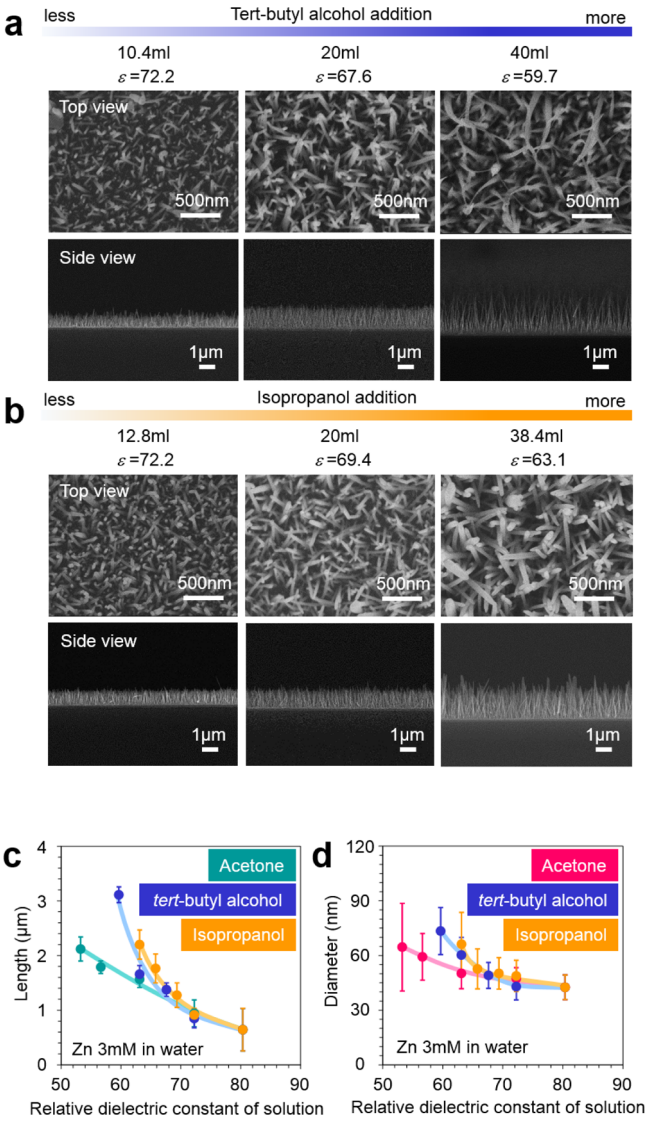

Figure 6. (a,b) Top view and side view FESEM images of ZnO nanowires grown in water−organic mixed solvents [(a) *tert*-butyl alcohol, (b) isopropanol] with varying the addition amount of organic solvents. The values of the relative dielectric constant of solution (ε) are also shown. (c,d) Statistically analyzed data of (c) length and (d) diameter of ZnO nanowires grown in various water−organic mixed solvents (acetone, *tert*-butyl alcohol, and isopropanol) as a function of the relative dielectric constant of solution. The Zn concentrations of all samples were controlled to be 3 mM in water prior to the addition of the organic solvent.

CONCLUSIONS

In conclusion, we demonstrated the effect of water−organic (acetone, *tert*-butyl alcohol and isopropanol) cosolvents on solution-based ZnO nanowire growth. The crystal growths of both length and diameter of nanowires were promoted by the addition of the organic solvent while the crystal growth nature and the optical properties of ZnO nanowires did not alter. We found that a variation of the relative dielectric constant in cosolvents critically determines the growth regime of ZnO nanowires. In addition, the so-called "solvent-sorting effect" is essential to understand the difference between different

DOI: 10.1021/acsomega.9b00945
ACS Omega 2019, 4, 8299−8304

organic solvents. This fundamental knowledge as to the effect of water−organic cosolvents will be a foundation to incorporate the water-insoluble chemicals into the nanowire and to synthesize novel inorganic−organic hybrid functional nanowires by simultaneously using water-compatible and organic-compatible chemical reagents.

EXPERIMENTAL SECTION

Solution based ZnO nanowire growth was performed using the water−organic cosolvent in an open system. For a growth substrate, a ZnO seed layer with a thickness of 50 nm was deposited onto the 20 mm × 20 mm SiO_2/Si substrate by radio frequency (rf) sputtering with a 50 W of rf power and 0.3 Pa of Ar pressure at room temperature. A thin Ti layer was inserted between the ZnO seed layer and the substrate to improve the adhesion. The growth solution of ZnO nanowires was prepared by dissolving equimolar hexamethylenetetramine and zinc nitrate hexahydrate ($Zn(NO_3)_2{\cdot}6H_2O$) in 100 mL deionized (DI) water by stirring, followed by the addition of organic solvents (acetone, *tert*-butyl alcohol, and isopropanol). The substrates with the ZnO seed layer were immersed into the growth solution in a manner of upside down. The beaker was then capped by a plastic wrap with small holes, which allowed us to maintain the pressure of the growth system constant by releasing the evaporated organic solvent during the growth process. The release of the evaporated organic solvent was delayed by re-condensing the solvents on the plastic wrap and dropping them into the growth solution. The nanowire growth was conducted for 20 h at 95 °C of the programmed oven temperature. To evaluate the effect of organic addition on temperature variation of the growth solution, the practical temperature of the growth solution was monitored during the growth process. Also an influence of the growth temperature on the crystal growth of ZnO nanowires was examined by varying the programmed oven temperature. After the nanowire growth, the samples were rinsed by DI water and blown by dry air. The relative dielectric constant values of water−organic cosolvents referred to the previous study.[30,31] The morphology, the crystal structure, and the defect property of fabricated ZnO nanowires were characterized by FESEM (JEOL JSM-7610F) at an acceleration voltage of 15 kV, TEM (JEOL JEM-2100F) at an acceleration voltage of 200 kV, XRD (Rigaku RINT-TTR III) and room temperature PL spectroscopy (JASCO FP-8500). The length and the diameter of ZnO nanowires were calculated by averaging 100 nanowires in FESEM images. To evaluate a variation of interfacial energy at the solvent/ZnO interface, the static CA of water−organic mixed solvent was measured on a single crystalline ZnO (0001) substrate by changing the mixing ratio of the organic solvent. The CA was measured at 10 s after dropping the solvent.

AUTHOR INFORMATION

Corresponding Authors

*E-mail: kazu-n@cm.kyushu-u.ac.jp (K.N.).
*E-mail: yanagida@cm.kyushu-u.ac.jp. Phone: +81-92-583-7621. Fax: +81-92-583-8820 (T.Y.).

ORCID

Kazuki Nagashima: 0000-0003-0180-816X
Takuro Hosomi: 0000-0002-5649-6696
Tsunaki Takahashi: 0000-0002-2840-8038
Takao Yasui: 0000-0003-0333-3559
Takeshi Yanagida: 0000-0003-4837-5701

Author Contributions

Y.A. and T.H., mainly conducted the experiments in this manuscript. Y.A., K.N., T.H., H.A., G.Z., and T.T. analyzed the results. The manuscript was written and revised by Y.A., K.N., T.H., M.K., T.Y., Y.B., and T.Y. All authors have given approval to the final version of the manuscript.

Notes

The authors declare no competing financial interest.

ACKNOWLEDGMENTS

This work was supported by KAKENHI (grant numbers nos. 18H01831, 18KK0112, 18H05243, 26220908, 17H04927, 17J09894) and CAS-JSPS Joint Research Projects (grant number no. GJHZ7891). K.N. and T.H. were supported by the MEXT Project of "Integrated Research Consortium on Chemical Sciences". T.Y. was supported by CREST of Japan Science and Technology Corporation (JST) and ImPACT. This work was performed under the Cooperative Research Program of "Dynamic Alliance for Open Innovation Bridging Human, Environment and Materials", and "Network Joint Research Center for Materials and Devices". K.N. acknowledges MUKAI Science and Technology Foundation for financial support. Y.A. acknowledges Takeshi Tanaka for his support of TEM observation and Taisuke Matsumoto for his support of XRD measurement.

REFERENCES

(1) Dhara, S.; Giri, P. K. ZnO Nanowire Heterostructures: Intriguing Photophysics and Emerging Applications. *Rev. Nanosci. Nanotechnol.* **2013**, *2*, 147−170.
(2) Qin, Y.; Wang, X.; Wang, Z. L. Microfibre-nanowire hybrid structure for energy scavenging. *Nature* **2008**, *451*, 809−813.
(3) Law, M.; Greene, Lori E.; Johnson, Justin C.; Saykally, R.; Yang, P. Nanowire dye-sensitized solar cells. *Nat. Mater.* **2005**, *4*, 455−459.
(4) Yasui, T.; Yanagida, T.; Ito, S.; Konakade, Y.; Takeshita, D.; Naganawa, T.; Nagashima, K.; Shimada, T.; Kaji, N.; Nakamura, Y.; Thiodorus, I. A.; He, Y.; Rahong, S.; Kanai, M.; Yukawa, H.; Ochiya, T.; Kawai, T.; Baba, Y. Unveiling massive numbers of cancer-related urinary-microRNA candidates via nanowires. *Sci. Adv.* **2017**, *3*, No. e1701133.
(5) Liu, C.; Tang, J.; Chen, H. M.; Liu, B.; Yang, P. A Fully Integrated Nanosystem of Semiconductor Nanowires for Direct Solar Water Splitting. *Nano Lett.* **2013**, *13*, 2989−2992.
(6) Dai, B.; Wang, J.; Xiong, Z.; Zhan, X.; Dai, W.; Li, C.-C.; Feng, S.-P.; Tang, J. Programmable artificial phototactic microswimmer. *Nat. Nanotechnol.* **2016**, *11*, 1087−1092.
(7) Navarro, J. R. G.; Mayence, A.; Andrade, J.; Lerouge, F.; Chaput, F.; Oleynikov, P.; Bergström, L.; Parola, S.; Pawlicka, A. WO_3 Nanorods Created by Self-Assembly of Highly Crystalline Nanowires under Hydrothermal Conditions. *Langmuir* **2014**, *30*, 10487−10492.
(8) Comini, E. Metal oxide nanowire chemical sensors: innovation and quality of life. *Mater. Today* **2016**, *19*, 559−567.
(9) Huang, M. H.; Mao, S.; Feick, H.; Yan, H.; Wu, Y.; Kind, H.; Weber, E.; Russo, R.; Yang, P. Room-Temperature Ultraviolet Nanowire Nanolasers. *Science* **2001**, *292*, 1897−1899.
(10) Wang, X.; Song, J.; Liu, J.; Wang, Z. L. Direct-Current Nanogenerator Driven by Ultrasonic Waves. *Science* **2007**, *316*, 102−105.
(11) Liu, C.; Dasgupta, N. P.; Yang, P. Semiconductor Nanowires for Artificial Photosynthesis. *Chem. Mater.* **2014**, *26*, 415−422.
(12) Zhang, J.; Tu, J.-P.; Xia, X.-H.; Wang, X.-L.; Gu, C.-D. Hydrothermal synthesized WO_3 nanowire arrays with highly improved electrochromic performance. *J. Mater. Chem.* **2011**, *21*, 5492−5498.

DOI: 10.1021/acsomega.9b00945
ACS Omega 2019, 4, 8299−8304

(13) Xu, S.; Wang, Z. L. One-Dimensional ZnO Nanostructures: Solution Growth and Functional Properties. *Nano Res.* **2011**, *4*, 1013−1098.
(14) Klamuchuen, A.; Suzuki, M.; Nagashima, K.; Yoshida, H.; Kanai, M.; Zhuge, F. W.; He, Y.; Meng, G.; Kai, S.; Takeda, S.; Kawai, T.; Yanagida, T. Rational Concept for Designing Vapor-Liquid-Solid Growth of Single Crystalline Metal Oxide Nanowires. *Nano Lett.* **2015**, *15*, 6406−6412.
(15) Zhu, Z.; Suzuki, M.; Nagashima, K.; Yoshida, H.; Kanai, M.; Meng, G.; Anzai, H.; Zhuge, F.; He, Y.; Boudot, M.; Takeda, S.; Yanagida, T. Rational Concept for Reducing Growth Temperature in Vapor-Liquid-Solid Process of Metal Oxide Nanowires. *Nano Lett.* **2016**, *16*, 7495−7502.
(16) Joo, J.; Chow, B. Y.; Prakash, M.; Boyden, E. S.; Jacobson, J. M. Face-selective electrostatic control of hydrothermal zinc oxide nanowire synthesis. *Nat. Mater.* **2011**, *10*, 596−601.
(17) Richardson, J. J.; Lange, F. F. Controlling Low Temperature Aqueous Synthesis of ZnO. 1. Thermodynamic Analysis. *Cryst. Growth Des.* **2009**, *9*, 2570−2575.
(18) Qiu, J.; Li, X.; Zhuge, F.; Gan, X.; Gao, X.; He, W.; Park, S.-J.; Kim, H.-K.; Hwang, Y.-H. Solution-derived 40μm vertically aligned ZnO nanowire arrays as photoelectrodes in dye-sensitized solar cells. *Nanotechnology* **2010**, *21*, 195602.
(19) Tian, Z. R.; Voigt, J. A.; Liu, J.; Mckenzie, B.; Mcdermott, M. J.; Rodriguez, M. A.; Konishi, H.; Xu, H. Complex and oriented ZnO nanostructures. *Nat. Mater.* **2003**, *2*, 821−826.
(20) Gu, Z.; Zhai, T.; Gao, B.; Sheng, X.; Wang, Y.; Fu, H.; Ma, Y.; Yao, J. Controllable Assembly of WO_3 Nanorods/Nanowires into Hierarchical Nanostructures. *J. Phys. Chem. B* **2006**, *110*, 23829−23836.
(21) Rojas, H. C.; Bellani, S.; Sarduy, E. A.; Fumagalli, F.; Mayer, Matthew T.; Schreier, M.; Grätzel, M.; Di Fonzo, F.; Antognazza, M. R. All Solution-Processed, Hybrid Organic-Inorganic Photocathode for Hydrogen Evolution. *ACS Omega* **2017**, *2*, 3424−3431.
(22) Tokudome, Y.; Morimoto, T.; Tarutani, N.; Vaz, P. D.; Nunes, C. D.; Prevot, V.; Stenning, G. B. G.; Takahashi, M. Layered Double Hydroxide Nanoclusters: Aqueous, Concentrated, Stable, and Catalytically Active Colloids toward Green Chemistry. *ACS Nano* **2016**, *10*, 5550−5559.
(23) Wen, B.; Huang, Y.; Boland, J. J. Controllable Growth of ZnO Nanostructures by a Simple Solvothermal Process. *J. Phys. Chem. C* **2008**, *112*, 106−111.
(24) Clavel, G.; Willinger, M.-G.; Zitoun, D.; Pinna, N. Solvent Dependent Shape and Magnetic Properties of Doped ZnO Nanostructures. *Adv. Funct. Mater.* **2007**, *17*, 3159−3169.
(25) Liu, B.; Zeng, H. C. Hydrothermal Synthesis of ZnO Nanorods in the Diameter Regime of 50 nm. *J. Am. Chem. Soc.* **2003**, *125*, 4430−4431.
(26) Das, K.; Panda, S. K.; Chaudhuri, S. Solvent-controlled synthesis of TiO2 1D nanostructures: Growth mechanism and characterization. *J. Cryst. Growth* **2008**, *310*, 3792−3799.
(27) He, Y.; Yanagida, T.; Nagashima, K.; Zhuge, F.; Meng, G.; Xu, B.; Klamchuen, A.; Rahong, S.; Kanai, M.; Li, X.; Suzuki, M.; Kai, S.; Kawai, T. Crystal-Plane Dependence of Critical Concentration for Nucleation on Hydrothermal ZnO Nanowires. *J. Phys. Chem. C* **2013**, *117*, 1197−1203.
(28) Anzai, H.; Suzuki, M.; Nagashima, K.; Kanai, M.; Zhu, Z.; He, Y.; Boudot, M.; Zhang, G.; Takahashi, T.; Kanemoto, K.; Seki, T.; Shibata, N.; Yanagida, T. True Vapor-Liquid-Solid Process Suppresses Unintentional Carrier Doping of Single Crystalline Metal Oxide Nanowires. *Nano Lett.* **2017**, *17*, 4698−4705.
(29) Suzuki, M.; Hidaka, Y.; Yanagida, T.; Klamchuen, A.; Kanai, M.; Kawai, T.; Kai, S. Essential role of catalyst in vapor-liquid-solid growth of compounds. *Physical Review E: Statistical, Nonlinear, and Soft Matter Physics* **2011**, *83*, 061606.
(30) Akerlof, G. Dielectric Constants of Some Organic Solvent-Water Mixtures at Various Temperatures. *J. Am. Chem. Soc.* **1932**, *54*, 4125−4139.
(31) Young, T. III. An Essay on the Cohesion of Fluids. *Philos. Trans. R. Soc. London* **1805**, *95*, 65−87.
(32) Owen, B. B. The Medium Effect of Various Solvents upon Silver Bromate at 25°. *J. Am. Chem. Soc.* **1933**, *55*, 1922−1928.
(33) Clever, H. L.; Verhoek, F. H. The Solubility of cis- and trans-Dinitrotetramminecobalt (III) and cis- and trans-Dinitrotetramminecobalt (III) dl-Dinitroöxalatodiammine Cobaltate in Dioxane−Water, Ethanol−Water and Acetone−Water Mixed Solvents at 15 and 25°. *J. Phys. Chem.* **1958**, *62*, 1061−1064.
(34) Ricci, J. E.; Nesse, G. J. Solubility of Potassium Iodate and Zinc Iodate in Dioxane-Water Mixtures; Effect of Sorting of Solvent Molecules. *J. Am. Chem. Soc.* **1942**, *64*, 2305−2311.
(35) Bulter, J. A. V. The Energy and Entropy of Hydration of Organic Compounds. *Trans. Faraday Soc.* **1937**, *33*, 229−236.

DOI: 10.1021/acsomega.9b00945
ACS Omega 2019, 4, 8299−8304